COHERENT STRUCTURES AND BUBBLE-PARTICLE VELOCITY IN 2-D FLUIDIZED BEDS

S. Sánchez-Delgado*, J.A. Almendros-Ibáñez, A. Soria-Verdugo, D. Santana and U. Ruiz-Rivas

ISE Group, Thermal and Fluid department, Universidad Carlos III de Madrid, Avda. de la Universidad 30, 28911 Leganés, Madrid, Spain

Abstract: This work presents an experimental study to characterize ascending bubbles and granular velocity in the dense phase of a 2-D fluidized bed. Three different non-intrusive techniques based on images obtained with a high speed camera are developed, and applied to the images. First the bubble paths are characterized with time-average concentration maps and the bubble velocities are obtained, using a tracking algorithm over the mass centers of the bubbles. Finally, a PIV (particle image velocimetry) method is used to characterize the particle velocity vectors. This procedure is repeated for different bed aspect ratios, and different superficial gas velocities. This study analyzes the superficial gas velocity influence on the bed behavior, and how the bubble path configuration depends on the bed aspect ratio. The PIV measurements give us information on the location of the recirculation regions and the influence of the superficial gas velocity.

INTRODUCTION

Fluidized beds are widely used in many industrial processes due to their high mixing capacity. In a gas-solid system, an increase in flow rate beyond minimum fluidization can change the internal structure of the bed: the coherent structures change, the coalescence phenomenon is more significant and bubble velocity grows within the bed. Therefore, the particle transport phenomena are more relevant recirculation regions change their size and location.

There have been several studies of bubble spatial distribution in fluidized beds. Tzeng et al. (1993), used a two-dimensional column to study the macroscopic flow structures of gas-liquid and gas-liquid-solid fluidization systems with flow visualization techniques, examining the effect of particle size, inlet liquid velocity and gas flow distribution. Other technique, based on tracking a phosphorescent tracer particle using a video recorder and digital image analysis has been used by Pallarés and Johnsson, (2005). Later on, Lim et al., (2006), used a gas-solid fluidized bed to observe the bubbling phase directly, using real time vision instrumentation. They obtained a contour plot of time-averaged spatial bubble residency depicting the bubble spatial distribution in a planar fluidized bed at steady state.

The aim of the present work is to identify the coherent structures present in a 2-D fluidized bed, to gather information on the internal structure in the bubbling regime, based on visualization techniques and PIV. We have measured the bubble distribution, bubble and particle velocity, the position of recirculation region, and the influence of bed aspect ratio and superficial gas velocity on the flow structure of the bed.

DATA COLLECTION & PROCESSING

The experiments were carried out in a 2-D cold fluidized bed of dimensions 10x60x0.5cm. A detailed description of the facility can be found in Almendros-Ibáñez et al., 2006. The air distributor was formed by 9 holes (1 mm diameter), with a 1 cm gap between them. The walls were made of glass and the back glass of the bed was recovered by a black card to generate more contrast in the images. The bed was filled with Geldart-B glass particles (Geldart, 1973) of 2500 kg/m^3 density ρ_p, and 300-400 μm diameter d_p.

Two operational variables were taken into account to define the experiments characteristics: the ratio between fixed bed height, h, and the bed width, w (0.5 and 1) and the ratio between the

superficial gas velocity, U, and the minimum fluidization velocity, U_{mf} (1.2, 1.4 and 1.6). Table 1 shows the six different cases tested.

Case	*h (m)*	*W (m)*	*h/w*	U_{mf} *(m/s)*	U/U_{mf}
1	0.05	0.1	0.5	1.6	1.2
2	0.05	0.1	0.5	1.6	1.4
3	0.05	0.1	0.5	1.6	1.6
4	0.1	0.1	1	3	1.2
5	0.1	0.1	1	3	1.4
6	0.1	0.1	1	3	1.6

Table 1: Different cases for different variables values (h,U)

Two spotlights of 650 watts were necessary to get a uniform illumination of the bed. A high speed video camera, *Redlake Motion pro X3*, with 4 Gb memory was used to take 3271 images at 125 frames per second. The image resolution varied for different bed aspect ratios: 789x1098 for h/w = 0.5, and 554x1277 for h/w = 1. From these data two 100-measurement samples were defined. Both samples were homogenously spaced along the data and set consecutively, as shown in table 2.

	Number of measurement				
Sample 1	1	34	67	…	3268
Sample 2	2	35	68	…	3269

Table 2: Samples obtained from the experimental data

These samples were used for all the following analyses. First, a visualization analysis is carried out. Sample 1 images are processed, calculating a threshold level for each one, to obtain a clear difference between particles (level = 1) and air (level = 0). The images of sample 1 were then summed and rescaled. Therefore, a time-averaged concentration map is obtained where solids and bubbles locations are defined. A rather similar analysis has been performed by Lim et al. 2006.

Secondly, the bubble mass centers and their velocities are obtained using the information in both samples. The mass centers in each image were identified using a computer code based on contour analysis. A max-min area criterion was established to reject outliers, as the highest area in each picture was the freeboard, and the lower areas are very likely to be shadow regions that appear close to the walls.

Then, to identify the mass center displacement for each recognized bubble in each image we use a method similar to the one explained in Rodríguez-Rodríguez et al., 2003. The bubbles on each image of the first sample were transformed in a circle of radius $\lambda * Req$, based in the bubble area. Then, the bubble mass centers on each image of the second sample are compared with the information of the correlating image of the first sample (2 with 1, 35 with 34, etc.) and those centers that lay inside of these circles were identified. The parameter λ was chosen so the probability to find the bubble mass center will be higher than 0.95, resulting in a value of 0.8. Sometimes, there were several points inside each circle; in those cases the bubble with a most similar area was selected. As a result of this procedure, pairs of centers on consecutive images are obtained. Knowing the bubble displacement and time delay between frames the bubble velocity can be computed.

Finally, using a PIV technique, the particle velocity field of each image was calculated. If the PIV images are summed, the time-average particle velocity vector map will be obtained.

RESULT AND DISCUSSION

Time-average concentration map

The results obtained for all cases in table1 are represented in figure 1, identifying the solid and air regions. In cases 1 and 4, a non uniform distribution of air in the fluidized bed is observed. The distributor is continuously supplying air along the width, but the bubble air flow is only visualized at the bottom right of the bed. Both cases correspond to a low excess gas velocity. A higher value of excess gas velocity gives a more uniform bubble distribution within the fluidized bed. In those cases the value of *h/w* influences the internal structure of the bed. Cases 2 and 3 (*h/w* = 0.5) show an important solid concentration effect in the walls and in the center of the bed, it generates two bubble paths completely separated with no coalescence effect between them. In cases 5 and 6 (*h/w* = 1) the two bubble paths join before the bubbles reach the bed surface, this effect generates only one big air channel in the center of the bed displacing the particles to the walls. Therefore, a high rate between height and width makes change the preferred paths of bubbles in fluidized beds even if superficial gas velocity keeps constant. This is in agreement with the well-known model of Werther and Molerous (1973, their figure 16).

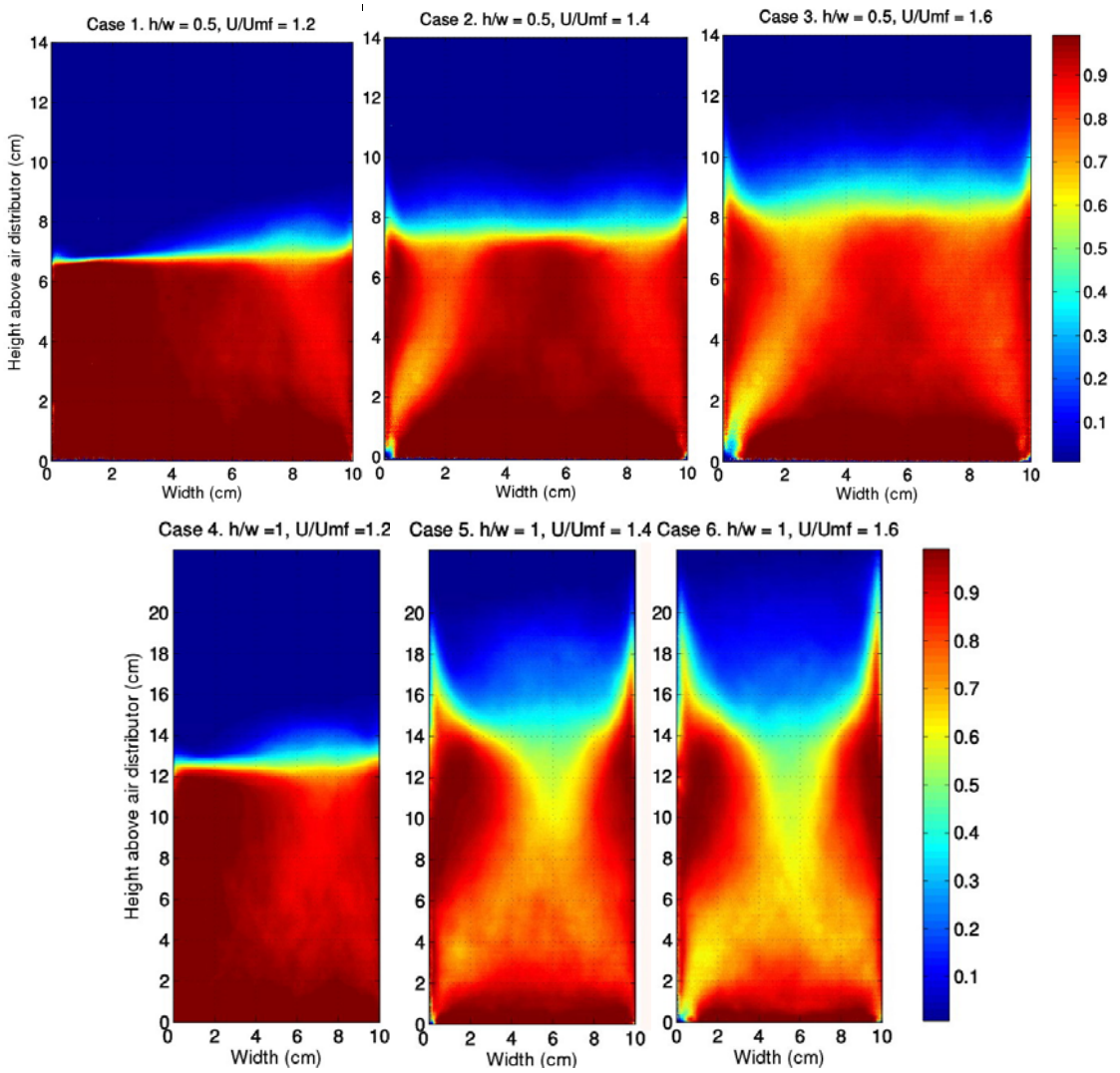

Fig. 1: Concentration maps for the six cases of summed images.

In order to quantify the visual observations of figure 1, time-average concentration profiles have been analyzed at bed heights close to the freeboard, *z*. Two of these profiles for cases 2 and 5, at *z* = 6 cm and *z* = 11 cm, respectively, are presented in figure 2. Both cases correspond to the same excess gas. The height-width ratio has an important effect in the circulation pattern found in the fluidized bed.

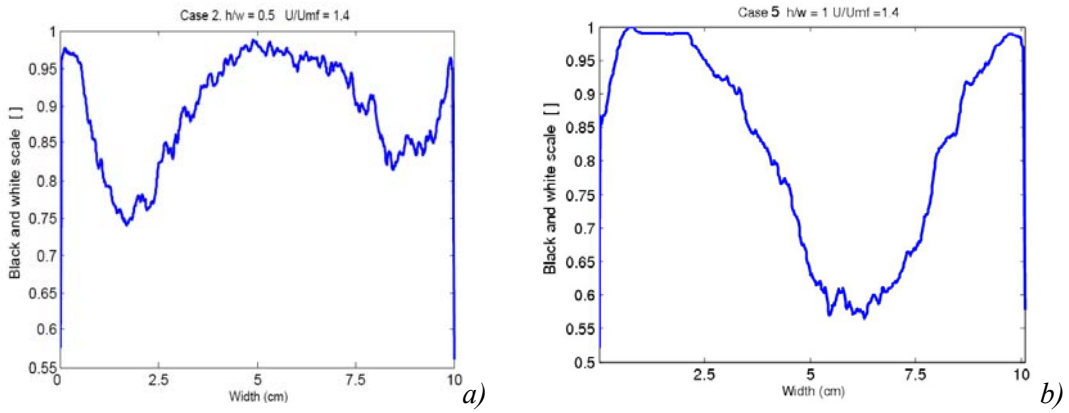

Fig. 2: Particle concentration profile near the freeboard in case 2 at z = 6 cm, and case 5 at z = 11cm.

Bubble mass center and bubble velocity

When images were analyzed, mass center coordinates of identified bubbles in each image of both samples were stored. With this information and the criterion explained in the previous section, the bubbles velocity vectors were calculated. Figure 3 shows the velocity vector corresponding to the motion of the mass center of the bubbles. The graphs are superposed to the bubble concentration maps (in grey scale, large bubble concentrations are shown in black and large particle concentrations in white).

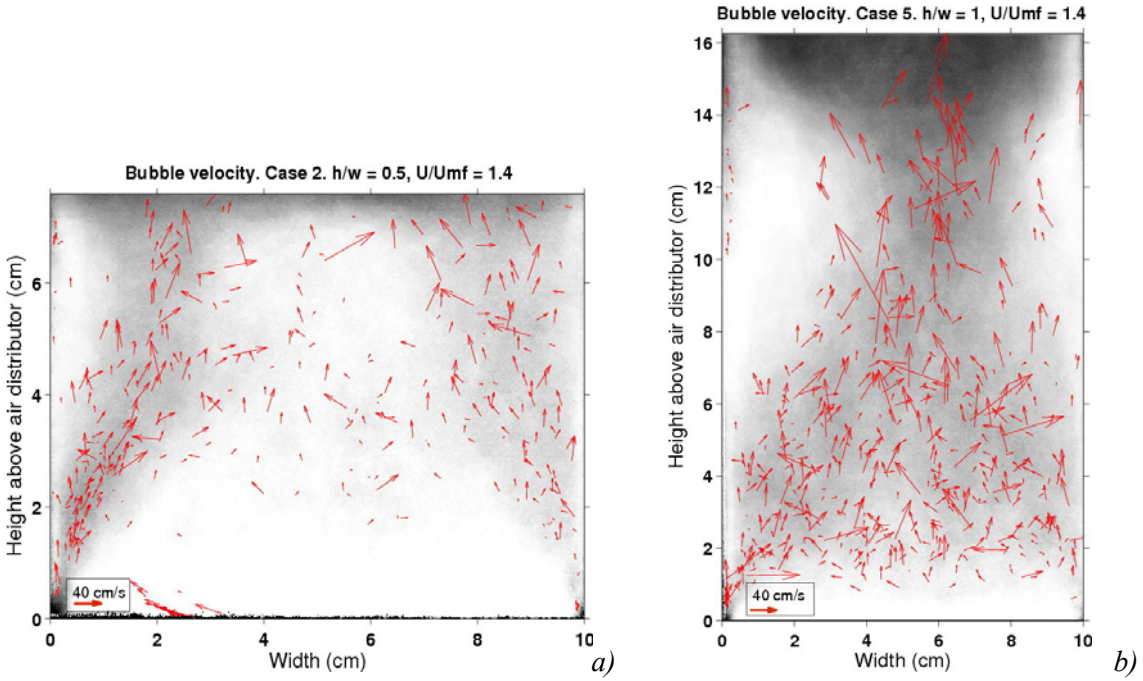

Fig. 3: Bubble concentration distribution and bubble velocity vectors for cases 2(a) and 5(b)

In both cases, the mass center distribution agrees well with the bubble concentration. Besides, figure 3 shows that the bubble velocities increase as the height above the distributor increases. This observation is consistent with the bubble coalescence and bubble velocity increase along the bed height.

Particles velocity, recirculation region and streamlines

Finally, the particle velocity fields were obtained using the PIV technique over correlating images of samples 1 and 2. The values obtained for each pair of images were summed obtaining the time-average particle velocity field along the bed, this procedure was applied for the six experimental cases. Figure 4, shows the particle velocities distribution for cases 2 and 5.

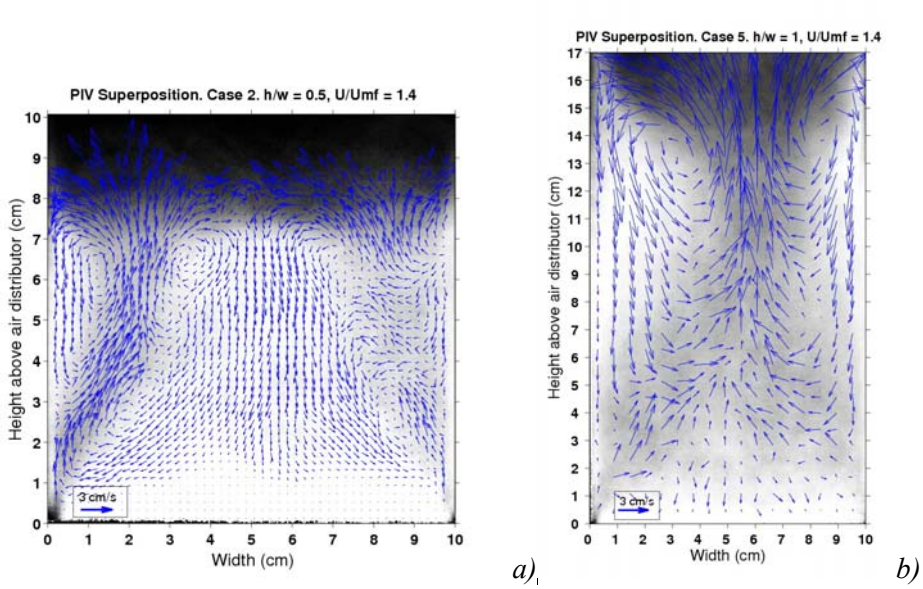

Fig. 4: PIV results for case 2 and case 5, a) b) respectively

The particle velocity vectors describe the transport phenomenon induced by ascending bubbles from the bottom to the top of the bed, and how the particle velocity increases by the bubble coalescence. Figure 5 shows zoom-in zones of interest where the recirculation centers are identified. One recirculation center can be see for case 2 (figure 5a), and two recirculation centers are identified at higher *h/w* shown in figure 5.b.

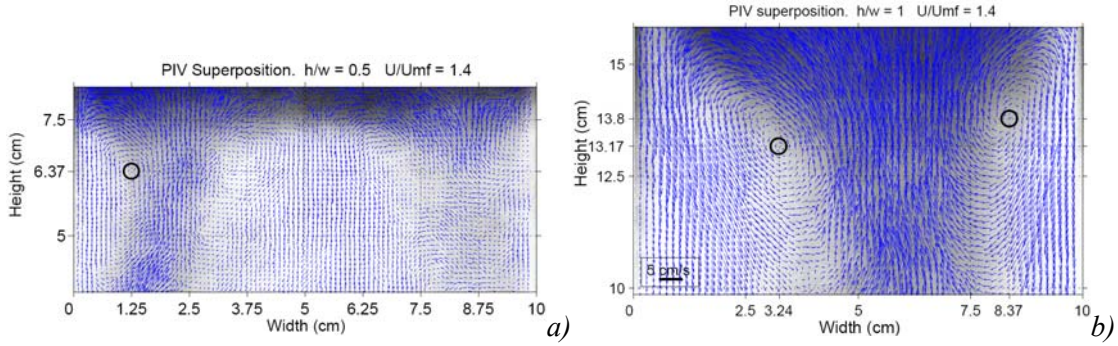

Fig. 5: Center of recirculation region in cases 2 and 5, a) b) respectively

In figure 6, the streamlines for previous cases are represented, where it is possible to observe how the origin of the streamlines fit with the recirculation region center.

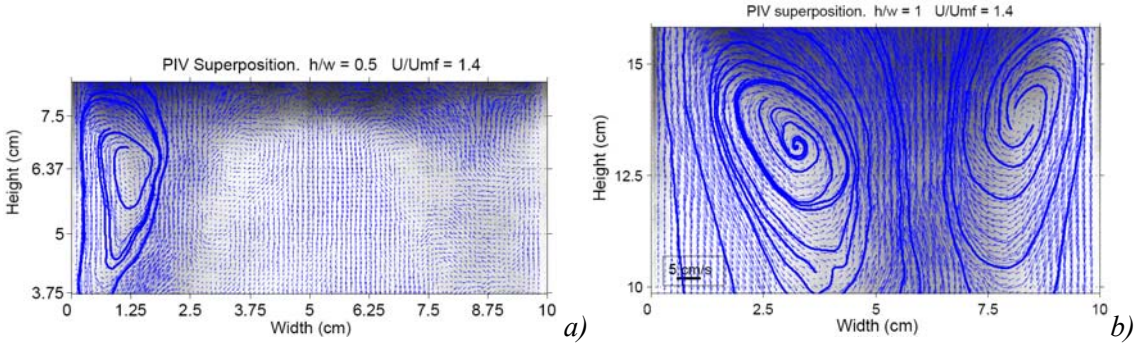

Fig 6: Streamlines around recirculation region, for cases 2 and 5 respectively.

When the air supply increases, the position of the recirculation regions centers change. If we continue increasing the gas supply and *U* exceed the terminal velocity of the particles, the recirculation regions will detach from the walls and the particle will be transported in the

pneumatic transport regime (Kunii and Levenspiel, 1991). Figure 7 shows the displacement of the recirculation region center when the superficial gas velocity increases.

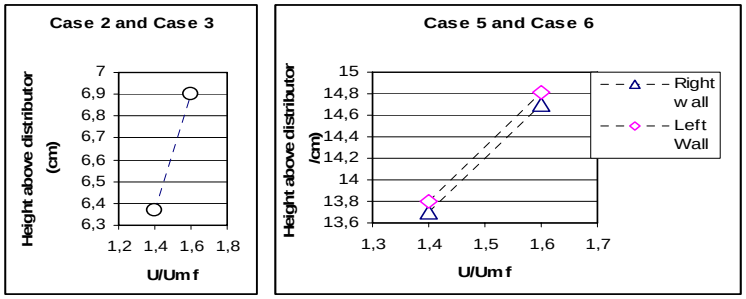

Fig. 7: Recirculation center position above air distribution, for different superficial gas velocities

CONCLUSION

An analysis technique has been developed to study the influence of the bed aspect ratio and the superficial gas velocity in the coherent structures formation. The techniques include the measurement and visualization of the bubble distribution, bubble velocity and particle velocity. This analysis shows the time-average behavior of the bed, and gives information about the bubble distribution. The bed aspect ratio is a very important parameter, as it permits or precludes the coalescence of large bubbles. The superficial gas velocity also plays an important role: if the superficial gas velocity increases with a constant bed aspect ratio, a bad distributed bed can change its structure and become in a more uniform air distribution along the fluidized bed.

NOTATION

ρ_p: particle density, kg/m^3
d_p: particle diameter, m
h: fixed bed height, cm
Req: equivalent radius of the bubble
U: Superficial gas velocity, m/s
U_{mf}: minimum fluidization velocity, m/s
w: fluidized bed width, cm
z: height above distributor, cm

REFERENCES

-Almendros-Ibáñez J.A, Sobrino C., de Vega M. and Santana D., 2006. A new model for ejected particle velocity from erupting bubbles in 2-D fluidized beds. Chemical Engineering Science, 61 5981-5990
-Geldart, D., 1973. Types of gas fluidization. Powder Technology, 7, 285-292
-Kunii D. Levenspiel O. Fluidization Engineering, 2nd Edition 1991. Butterworth-Heinemann
-Lim C.N, Gilberston M.A and Harrison A.J.L., 2006. Bubble distribution and behaviour in bubbling fluidised beds. Chemical Engenieering Science, 62 56-59
-Pallarés D. and Johnsson F. 2006. A novel technique for particle tracking in cold 2-dimensional fluidized beds-simulating fuel dispersión. Chemical Engineering Science 61 2710 – 2720
-Rodríguez-Rodríguez J, Martínez-Bazán C. and Montañes J.L. 2003. A novel particle tracking and break-up detection algorithm: application to the turbulent break-up of bubbles. Measurements Science and Technology 14 1328-1340
-Werther J. and Molerus O. 1973. The local structure of gas fluidized beds-II. The spatial distribution of bubbles. Int. J. Multiphase Flow, 1 123-138.
-Tzeng J.W., Chen R.C., and Fan L.S. 1993. Visualization of flow characteristics in a 2-D bubble column and three phase fluidized bed. AIChe Journal, 39 5

ACKNOWLEDGMENTS

This work has been partially supported by the National Energy Program of the Spanish Department of Science and Education and the Madrid Community under the project numbers ENE2006-01401 and CCG06-UC3M/ENE-0764 respectively.